Eur. Phys. J. A **17**, 133–144 (2003)
DOI 10.1140/epja/i2002-10140-7

THE EUROPEAN PHYSICAL JOURNAL A

Final-state interaction in semi-inclusive DIS off nuclei

C. Ciofi degli Atti[1,a] and B.Z. Kopeliovich[2,3,b]

[1] Department of Physics, University of Perugia, and INFN, Sezione di Perugia, via A. Pascoli, Perugia, I-06100, Italy
[2] Max-Planck-Institut für Kernphysik, Postfach 103980, 69029 Heidelberg, Germany
[3] Institut für Theoretische Physik der Universität, 93040 Regensburg, Germany

Received: 28 June 2002 / Revised version: 6 October 2002 /
Published online: 5 May 2003 –
Communicated by A. Schäfer

Abstract. The Final-State Interaction (FSI) in Deep-Inelastic Scattering (DIS) of leptons off a nucleus A, due to the propagation of the struck nucleon debris and its hadronization in the nuclear environment is considered. The effective cross-section of such a partonic system with the nucleons of the medium and its time dependence are estimated, for different values of the Bjorken scaling variable, on the basis of a model which takes into account both the production of hadrons due to the breaking of the color string, which is formed after a quark is knocked out off a bound nucleon, as well as the production of hadrons originating from gluon radiation. It is shown that the interaction, the evolution and the hadronization of the partonic system in the nuclear environment can be thoroughly investigated by a new type of semi-inclusive process, denoted $A(e,e'(A-1))X$, in which the scattered lepton is detected in coincidence with a heavy nuclear fragment, namely a nucleus $(A-1)$ in low energy and momentum states. As a matter of fact, if the FSI is disregarded, the momentum distribution of $(A-1)$ is directly related to the momentum distribution of the nucleon before γ^* absorption, *i.e.* the same quantity which appears in the conventional $A(e,e'N)X$ process, where N denotes a nucleon. The rescattering of the struck nucleon debris with the medium damps and distorts the momentum distributions of $(A-1)$ in a way which is very sensitive to the details of the effective cross-section of the debris with the nucleons of the medium. The total cross-section of the process $A(e,e'(A-1))X$ on ^{4}He, ^{16}O, and ^{40}Ca, related to the probability that after a target nucleon experiences a DIS process, the recoiling $(A-1)$ nucleus remains intact in spite of the strong FSI, is evaluated, and the distorted momentum distribution of the recoiling $(A-1)$ system is obtained. It is shown that both quantities are very sensitive to the details of the early stage of hadronization of the nucleon debris in the nuclear medium.

PACS. 24.85.+p Quarks, gluons, and QCD in nuclei and nuclear processes – 25.10.+s Nuclear reactions involving few-nucleon systems – 25.30.Dh Inelastic electron scattering to specific states – 25.30.Fj Inelastic electron scattering to continuum

1 Introduction

Lepton scattering off nuclei in the Deep-Inelastic Scattering (DIS) regime represents a powerful tool to investigate a wide range of physics processes related to strong-interaction physics which are more difficult to study in lepton scattering off free nucleons. As a matter of fact, in lepton nucleus scattering the interaction of the debris of the struck nucleon with the nuclear medium during the hadronization processes, could provide in principle valuable information on the space-time structure of the hadron formation mechanism (see, *e.g.*, [1]). Among others, we should stress two main motivations for thoroughly investigating quark interaction in the hadronic medium:

1. the first one, as already pointed out, is related to the possibility to understand the very mechanism and space-time development of hadronization, especially at its early stage; as different from experiments with inclusive hadron production in DIS [1] processes, with a recoil intact $(A-1)$ nucleus are not contaminated by hadronic cascades in nuclear matter;
2. the second one stems from the obvious necessity, once a workable model for quark propagation and hadronization is developed, to apply it to the treatment the Final-State Interaction (FSI) in various processes involving nuclei, like, *e.g.*, ultra-relativistic heavy-ion collisions, aimed at observing a possible quark-gluon plasma formation, and semi-inclusive lepton DIS scattering processes, aimed at investigating

[a] e-mail: ciofi@pg.infn.it
[b] e-mail: bzk@pluto.mpi-hd.mpg.de

possible distortions of the nucleon structure function of a bound nucleon (EMC effect).

It is the aim of this paper to update a comprehensive and workable model to treat the propagation and re-interaction in the medium of a nucleon debris produced in a DIS process off a bound nucleon [2], and to apply it to a recently proposed semi-inclusive DIS process on nuclei [3], which could be useful not only to investigate in a more detailed way the mechanism of formation length and hadronization, but also to obtain more reliable information on EMC-type effects.

To date, the information on hadron formation length comes mainly from the measurement of the multiplicity ratio of the lepto-produced hadrons in semi-inclusive $A(e,e'h)X$ processes [4–6], whose interpretation, on the basis of the quark re-interaction model we consider in this paper [2], appeared to be very convincing (see, *e.g.*, [7] for a discussion of recent HERMES data). However, it should also be pointed out that more exclusive processes, *e.g.* of the type we are going to discuss, though difficult to perform, could in principle provide more direct information on quark re-interaction and hadronization mechanisms. As for the EMC-type effects, in spite of many experimental and theoretical efforts (for a recent review see [8]), the origin of the nuclear EMC effect has not yet been fully clarified, and the problem as to whether, and to which extent, the quark distributions of nucleons undergo deformations due to the nuclear medium, remains open. This is why various semi-inclusive experiments in which another particle is detected in coincidence with the scattered electron have been proposed. Most of theoretical studies in this field concentrated on the process $D(e,e'N)X$, where D denotes the deuteron, N a nucleon, and X the undetected hadronic state. Current theoretical models of this process are based upon the *Impulse Approximation* (IA) (or the *the spectator model*), according to which i) X results from DIS off one of the two nucleons in the deuteron, ii) the second nucleon N recoils without interacting with X and is detected in coincidence with the scattered electron (for an exhaustive review see [9]). The model has been improved by considering that the detected nucleon could also originate from quark hadronization [10,11], and has also been extended to complex nuclei by considering the process $A(e,e'N)X$, by assuming that DIS occurs on a nucleon of a correlated pair, with the second nucleon N recoiling and detected in coincidence with the scattered electron [11].

In all the above calculations, however, the nucleon debris created by the virtual photon is assumed to propagate without re-interacting with the spectator nucleus, which, therefore, always remains intact, an assumption which, at first sight, might appear unjustified.

As a matter of fact, DIS off a bound nucleon results in the production of a multi-particle final state with an effective mass squared equal to

$$\begin{aligned} s' &\simeq m_N^2 - Q^2 + 2\,m_N\,\nu - 2\,\sqrt{\nu^2 - Q^2}\,p_{\rm L} \\ &= Q^2\left(\frac{1}{x} - 1\right) + m_N^2 - 2|\mathbf{q}|p_{\rm L}\,, \end{aligned} \tag{1}$$

where $Q^2 = \mathbf{q}^2 - \nu^2$ is the four-momentum transfer, ν the virtual photon energy in the rest frame of the nucleus, $p_{\rm L}$ the longitudinal Fermi momentum of the nucleon relative to the direction of the virtual photon ($\mathbf{q} \parallel z$), m_N the nucleon mass, and $x = \dfrac{Q^2}{2m_N\nu}$ the Bjorken scaling variable (we neglect here the binding energy of the nucleon). At high energies and far from the quasi-elastic region ($x \approx 1$), the effective mass is large, $\sqrt{s'} \gg m_N$, and one could expect the production of many particles which can interact traveling through the nucleus. This would substantially suppress the probability for the spectator nucleus to remain intact. However, the process of multi-particle production has a specific space-time development, and it turns out that not so many particles have a chance to be created inside the nucleus.

Recently [3], a new type of semi-inclusive process on complex nuclei has been considered, namely the process $A(e,e'(A-1))X$, in which DIS occurs on a mean-field, low-momentum nucleon, and the nucleus $(A-1)$, recoiling with low momentum and low excitation energy, is detected in coincidence with the scattered electron. Within the IA, it has been shown that such a process exhibits a series of very interesting features which could in principle provide useful insight on the nature and the relevance of quark FSI in DIS off nuclei, the validity of the spectator mechanism, and the medium-induced modifications of the nucleon structure function. In the present paper we go beyond the IA by considering the effects of the quark re-interaction in order to clarify i) to which extent the conclusions reached in ref. [3] will be affected by the FSI, and ii) if, and to which extent, the process is sensitive to the details of quark hadronization in nuclear environment.

Our paper is organized as follows: in sect. 2 the formalism of the FSI is presented; the application of the theory to the process $A(e,e'(A-1))X$ is illustrated in sect. 3; the results of calculations of the total cross-section and the distorted momentum distributions are exhibited in sect. 4; the summary and conclusion are given in sect. 5.

2 Final-state interaction and hadronization in semi-inclusive processes

2.1 Coherence time for particle production. The color string model

After a quark is knocked out off a bound nucleon by the virtual photon, a color field is stretched between the quark and the remnants of the nucleon. In the color flux tube model [12,13], one assumes that this process is adiabatic, *i.e.* gluon radiation is neglected while the color field is squeezed by the QCD vacuum to a color tube of a constant cross-area. Assuming that the transverse dimension of the tube is much smaller than its length one can call it color string.

The important parameter of the model is the string tension, *i.e.* the energy density per unit of length, which

is related to the hadronic mass spectrum [12],

$$\kappa = \frac{1}{2\,\pi\,\alpha'_{\rm R}} \simeq \frac{1\,{\rm GeV}}{\rm fm}\ , \tag{2}$$

where $\alpha'_{\rm R} \approx 0.9\,{\rm GeV}^{-2}$ is the slope of the leading Regge trajectories.

The energy of the leading quark degrades with a constant rate, $-{\rm d}E/{\rm d}z = \kappa$, ($z$ is the longitudinal coordinate) which is invariant relative to Lorentz boosts. At the same time, the rest of the nucleon (*e.g.*, a diquark) speeds up with the same acceleration, so the total momentum and energy of the debris of the nucleon remain constant. The string itself carries only energy, but no longitudinal momentum.

Naively, one might think about a long string stretched across the nucleus. However, the slow end of the string is accelerated and reaches soon the speed of the light. It turns out that the maximal length of the string in the rest frame of the target nucleon is

$$L_{\rm max} = \frac{m_{qq}}{\kappa}\ , \tag{3}$$

where m_{qq} is the mass of the rest of the nucleon, which we conventionally call a diquark. Assuming this mass to be less than the mass of the nucleon, one gets $L_{\rm max} < 1\,{\rm fm}$. Thus, the string propagating through the nucleus is rather a short object in the nuclear rest frame. Moreover, subsequent decays of the string via spontaneous $\bar{q}q$ pair production from vacuum make the string even shorter (see below).

Since the interaction cross-section of a high-energy colorless object in QCD depends only on its transverse size, one can assume that for such a string the cross-section should be of the order of nucleon-nucleon total cross-section.

An important phenomenon related to the string evolution is the spontaneous creation of quark-antiquark pairs from vacuum via the Schwinger mechanism. Since the string potential is a linear function of the distance, a created $\bar{q}q$ pair completely screens the external fields in between, therefore, it breaks the string into two pieces. If so, the interaction cross-section may nearly double compared to one string. This is important and must be taken into account.

The probability $W(t)$ for a string to create no quark pairs since its origin is given by

$$W(t) = \exp\left[-\,w\int\limits_0^t {\rm d}t'\,L(t')\right]\ , \tag{4}$$

where w is the probability rate to create a light $\bar{q}q$ pair within a unit of length of the string and a unit of time ($t = z$, in natural units), and $L(t)$ is the time-dependent length of the string. Note that eq. (4) is invariant relative to longitudinal Lorentz boosts.

The key parameter w can be estimated either using the Schwinger formula, or by calculating the decay width of heavy resonances [12,13], both ways giving $w \approx 2\,{\rm fm}^{-2}$. One can also evaluate w from the momentum distribution of the recoil protons in the reaction $pp \to pX$ [14,15]. If the final proton stays in the fragmentation region of the target, it acquires momentum due to the acceleration by the string up to the moment Δt of the first string breaking.

This moment is determined according to (4) by the condition

$$\frac{1}{2}\,w\,\Delta t^2 \approx 1\,. \tag{5}$$

The momentum which the proton gets during this time interval, $p = \kappa\,\Delta t$, is related to the Feynman $x_{\rm F}$ of the leading proton (in the anti-laboratory frame), $p = m_N\,(1 - x_{\rm F}^2)/2x_{\rm F}$. The mean value of $x_{\rm F}$ is known from data, $\langle x_{\rm F}\rangle \approx 0.5$. Therefore, $\langle p\rangle \approx 1\,{\rm GeV}/c$, and $w = 2/\Delta t^2 \approx 2\,\kappa^2/p^2 \approx 2\,{\rm fm}^{-2}$. Thus, all of these estimates converge at about the same value.

From this consideration we found that the mean time of breaking of the string after its production is $\Delta t \approx 1\,{\rm fm}$. Since after each breaking the leading piece of the string becomes twice shorter (in the lab frame), the time interval up to the next breaking, and correspondingly the momentum of the next produced particle, double. This is the way how string decay produces sequences of hadrons whose momenta are ordered in geometrical progression, corresponding to a plateau in rapidity scale. This bunch of particles with multiplicity rising with time propagates through nuclear matter with increasing probability to interact, *i.e.* to break up the recoiling nucleus. The effective interaction cross-section of the partonic system developing in nuclear matter rises as function of time as

$$\sigma_{\rm eff}(t) = \sigma_{\rm tot}^{NN} + \sigma_{\rm tot}^{MN}\,n_M(t)\ , \tag{6}$$

where

$$n_M(t) = \frac{\ln(1 + t/\Delta t)}{\ln 2}\ , \tag{7}$$

and we have assumed that the string at the early stage before the first breaking interacts with the nucleon cross-section. Subsequent decays of the string are assumed to be, ${\rm str} \to B + {\rm str} \to B + M + {\rm str} \to B + 2\,M + {\rm str}\ldots$, where B and M are baryon and meson, respectively. All other produced particles are mesons which are assumed to interact with the pionic cross-section, $\sigma_{\rm tot}^{MN} = \sigma_{\rm tot}^{\pi N}$. We also assume that they decay predominantly outside the nucleus. The latter assumptions is well justified for few-GeV mesons.

The effective cross-section (6) grows logarithmically with time and in a long time interval, $t \propto E_q$, when the hadronization is completed, reaches the maximal value

$$\sigma_{\rm max} \approx \sigma_{\rm tot}^{NN} + \sigma_{\rm tot}^{\pi N}\,\langle n_M\rangle\ , \tag{8}$$

where $\langle n_M\rangle$ is the observed mean multiplicity of produced mesons. If the energy of the quark initiating the jet is sufficiently high, the late stage of string hadronization happens outside the nucleus.

2.2 Gluon Bremsstrahlung

An intuitive QED analogy for the string model would be a capacitor whose plates are much larger than the distance

between them. These plates moving apart are losing energy mainly for the creation of the static electric field, while photon radiation from the edges is a small correction. This analogy gives a hint to the restrictions for the application of the string model. Probably, soft inelastic interactions can be treated this way, although the size of a constituent quark and the length of the color flux tube $\sim 1\,\mathrm{fm}$ (up to the first break) are of the same order, and gluon radiation might be an important correction. However, a quark knocked out by a highly virtual photon in DIS has size $\sim 1/Q$, much smaller than the length of the string. This is apparently a situation when the "edge effect" of gluon radiation plays a major role [2].

In order to estimate the effect of gluon radiation one can rely upon perturbative QCD methods [2,16,17]. We are interested in the time dependence of the amount of radiated gluons, therefore the coherence time of radiation is important. It depends on the quark energy which is about the energy of the incident virtual photon $E_q \approx \nu$, the transverse momentum k_T of the gluon, and the fraction α of the quark light-cone momentum it carries [2,16],

$$t_\mathrm{c} = \frac{2\,E_q\,\alpha\,(1-\alpha)}{k_\mathrm{T}^2 + \alpha^2\,m_q^2}\ , \tag{9}$$

where m_q is the quark mass which is not important for further estimates.

The mean number of gluons which lose coherence and are radiated during the time interval t is given by [2,18],

$$n_G(t) = \int\limits_{\lambda^2}^{Q^2} \mathrm{d}k_\mathrm{T}^2 \int\limits_{k_\mathrm{T}/E_q}^{1} \mathrm{d}\alpha\,\frac{\mathrm{d}n_G}{\mathrm{d}k_\mathrm{T}^2\,\mathrm{d}\alpha}\,\Theta(t-t_\mathrm{c})\ , \tag{10}$$

where the number of radiated gluons as a function of α and $\vec{k}_\mathrm{T}$ reads [2,19],

$$\frac{\mathrm{d}n_G}{\mathrm{d}\alpha\,\mathrm{d}k_\mathrm{T}^2} = \frac{4\alpha_s(k_\mathrm{T}^2)}{3\,\pi}\ \frac{1}{\alpha\,k_\mathrm{T}^2}\,. \tag{11}$$

Here $\alpha_s(k_\mathrm{T}^2) = 4\,\pi/9\,\ln(k_\mathrm{T}^2/\Lambda_\mathrm{QCD}^2)$ is the leading order QCD running coupling. We use the approximation of soft radiation, $\alpha \ll 1$ and $k_\mathrm{T}^2 \ll Q^2$. Since $\mathrm{d}n_G/\mathrm{d}k_\mathrm{T}^2 \propto 1/k^4$ at $k_\mathrm{T}^2 \gg Q^2$ [20], we can use Q^2 as the ultraviolet cut-off in the k_T^2 integration in eq. (10).

To avoid double counting we assume that at $Q < \lambda$ the string fragmentation mechanism dominates the nonperturbative dynamics of particle production. For this reason we introduced in (10) an infrared cut-off λ^2 for the k_T^2-integration, which should be taken of the order of the semi-hard scale characterizing gluon radiation. This scale was fixed in [17] at $\lambda = 0.65\,\mathrm{GeV}$ from data on diffractive gluon radiation (the triple-Pomeron mechanism) in soft hadronic collisions. The relatively large value of λ corresponding to a semi-hard scale, is dictated by the experimentally observed smallness of the cross-section of single diffraction, $pp \to pX$ to states of large effective mass M_X. The parameter λ controls the size of the virtual gluon clouds surrounding the valence quarks. Although the mean radius of the cloud $r_0 \simeq 0.3\,\mathrm{fm}$ might seem to be small, it goes well along with the radius of gluon-gluon correlation, calculated on the lattice [21], or with the instanton phenomenology [22] which gives similar estimates. The appearance of such a semi-hard scale has presumably a nonperturbative origin and was interpreted in [17] as a result of a strong nonperturbative light-cone potential between the parent quark and gluon.

After integration in (10) we find that the multiplicity of radiated gluons rises with time differently depending on whether t is smaller or larger than $t_0 = 1/(m_M\,x_\mathrm{Bj}) = 0.2\,\mathrm{fm}/x_\mathrm{Bj}$. At $t < t_0$,

$$n_G(t) = \frac{16}{27}\left\{\ln\left(\frac{Q}{\lambda}\right) + \ln\left(\frac{t\,\Lambda_\mathrm{QCD}}{2}\right)\ln\left[\frac{\ln(Q/\Lambda_\mathrm{QCD})}{\ln(\lambda/\Lambda_\mathrm{QCD}}\right]\right\}. \tag{12}$$

At $t > t_0$ the t-dependence starts leveling off,

$$\begin{aligned} n_G(t) = \frac{16}{27}\Bigg\{&\ln\left(\frac{Q}{\lambda}\,\frac{t_0}{t}\right) \\ &+ \ln\left(\frac{t\,\Lambda_\mathrm{QCD}}{2}\right)\ln\left[\frac{\ln(Q/\Lambda_\mathrm{QCD}\sqrt{t_0/t})}{\ln(\lambda/\Lambda_\mathrm{QCD})}\right] \\ &+ \ln\left(\frac{Q^2\,t_0}{2\,\Lambda_\mathrm{QCD}}\right)\ln\left[\frac{\ln(Q/\Lambda_\mathrm{QCD})}{\ln(Q/\Lambda_\mathrm{QCD}\,\sqrt{t_0/t})}\right]\Bigg\}, \end{aligned} \tag{13}$$

and reaches the maximal constant value when the time exceeds the full hadronization time, $t > t_0\,Q^2/\lambda^2$,

$$n_G^\mathrm{max} = \frac{16}{27}\left\{-\ln\left(\frac{Q}{\lambda}\right) + \ln\left(\frac{Q^2\,t_0}{2\Lambda_\mathrm{QCD}}\right)\ln\left[\frac{\ln(Q/\Lambda_\mathrm{QCD})}{\ln(\lambda/\Lambda_\mathrm{QCD})}\right]\right\}. \tag{14}$$

Apparently, all the three regimes eqs. (12)-(14) match.

Thus, we have arrived at a similar logarithmic growth of the amount of the produced particles with time as in the string model. Note that no gluons is radiated at $Q \to \lambda$, which is reasonable since at this value the onset of the nonperturbative dynamics of gluon radiation is expected [17]. At $Q > \lambda$ the amount of gluons slowly rises with Q. This observation does not contradict the fact that gluons provide the main contribution to the energy loss at large values of Q^2 [2]. Although the amount of hard (high-k_T) gluons is small, each of them takes away a large value of energy, $\omega > k_\mathrm{T}^2 t$.

One can replace each radiated gluon by a color octet $\bar{q}q$ pair with accuracy $1/N_\mathrm{c}^2$, and rearrange these pairs to form colorless $\bar{q}q$ dipoles. If to treat those dipoles as produced mesons, the effective cross-section (6) gets an extra contribution,

$$\sigma_\mathrm{eff}(t) = \sigma_\mathrm{tot}^{NN} + \sigma_\mathrm{tot}^{\pi N}\Big[n_M(t) + n_G(t)\Big]\ , \tag{15}$$

which smoothly switches into the expression (7) at $Q \to \lambda$. The effective absorption cross-section σ_eff as a function of time is depicted in fig. 1 for different values of x_Bj.

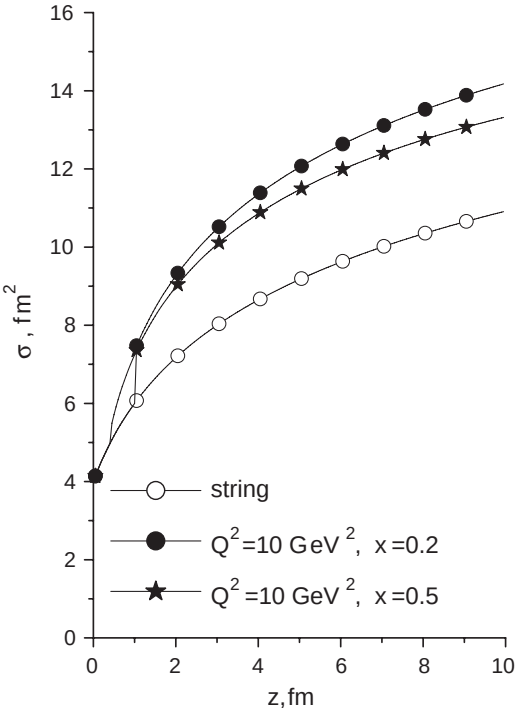

Fig. 1. The effective quark debris-nucleon cross-section *vs.* the longitudinal coordinate z in correspondence of $Q^2 = 10\,\mathrm{GeV}^2$ and two values of the Bjorken scaling variable x. The open dots correspond to the string model (eq. (6)), and the full dots and stars represents the total $\sigma_{\rm eff}$, *i.e.* the sum of the string and gluon radiation contributions (eq. (15)).

3 The semi-inclusive process A(e, e′(A − 1))X

3.1 The Impulse Approximation

The process we are going to consider is the one in which γ^*, interacting at high Q^2 with a quark of a mean-field nucleon (to be labeled by "1", and considered to be a proton), having four-momentum $p_1 \equiv (p_{10}, \vec{p_1})$, with $\vec{p_1} \equiv -\vec{P}_{A-1}$, creates a nucleon debris which propagates in the $A-1$ nucleon system, which recoils with low momentum $\vec{P}_{A-1}$ and low excitation energy, and is detected in coincidence with the scattered electron. We are interested in the propagation and interaction of the quark debris with the nuclear environment, but, to better understand the problem, we first analyze the *Impulse Approximation* (IA), when any kind of FSI is disregarded. In one-photon–exchange approximation, the differential cross-section in the laboratory system has the following form [3]:

$$\sigma_1^A(x, Q^2, \vec{P}_{A-1}) \equiv \sigma_1^A = \frac{\mathrm{d}\sigma^A}{\mathrm{d}x\mathrm{d}Q^2\mathrm{d}\vec{P}_{A-1}} = K^A(x, Q^2, y_A, z_1^{(A)}) z_1^{(A)} \times F_2^{N/A}(x_A, Q^2, p_1^2)\, P^A(E, |\vec{P}_{A-1}|), \quad (16)$$

where $Q^2 = -q^2 = -(k_e - k_e')^2 = \vec{q}^{\,2} - \nu^2 = 4E_eE_e'\sin^2\frac{\theta}{2}$ is the four-momentum transfer (with $\vec{q} = \vec{k}_e - \vec{k}_e'$, $\nu = E_e - E_e'$ and $\theta \equiv \theta_{\widehat{\vec{k}_e\vec{k}_e'}}$), $x = Q^2/2M\nu$ is the Bjorken scaling variable, $p_1 \equiv (p_{10}, \vec{p_1})$, with $\vec{p_1} \equiv -\vec{P}_{A-1}$, is the four momentum of the nucleon before the interaction with γ^*, $F_2^{N/A}$ the DIS structure function of a nucleon bound in nucleus A, and $K^A(x, Q^2, y_A, z_1^{(A)})$ the following kinematic factor:

$$K^A(x, Q^2, y_A, z_1^{(A)}) = \frac{4\alpha^2}{Q^4}\frac{\pi}{x}\cdot\left(\frac{y}{y_A}\right)^2\left[\frac{y_A^2}{2} + (1 - y_A) - \frac{p_1^2 x_{\rm Bj}^2 y_A^2}{z_1^{(A)2} Q^2}\right], \quad (17)$$

with

$$y = \nu/E_e\,, \qquad y_A = (p_1\cdot q)/(p_1\cdot k_e)\,, \quad (18)$$

$$x_A = \frac{x_{\rm Bj}}{z_1^{(A)}}\,, \qquad z_1^{(A)} = \frac{p_1\cdot q}{M\nu}\,. \quad (19)$$

In eq. (16), the quantity $P(E, |\vec{P}_{A-1}|)$ is the Nucleon Spectral Function

$$P^A(E, |\vec{P}_{A-1}|) = \sum_f |\langle \vec{P}_{A-1}, \Psi_{A-1}^f | \Psi_A^0\rangle|^2 \delta\big(E - (E_{\rm min} + E_{A-1}^f)\big) \quad (20)$$

where Ψ_A^0 and Ψ_{A-1}^f are the wave functions of the target nucleus and the final nucleus $(A-1)$ in the excited intrinsic state f, respectively, $E = E_{\rm min} + E_{A-1}^f$ is the nucleon removal energy, *i.e.* the energy required to remove a nucleon from the target, leaving the $(A-1)$ nucleus with excitation energy E_{A-1}^f, and, eventually, $E_{\rm min} = M + M_{A-1} - M_A$.

From now-on, the overlap appearing in eq. (20) will be called the *transition form factor* of the process and will be denoted as follows:

$$F_{A-1,A}^f(\vec{P}_{A-1}) \equiv \langle \vec{P}_{A-1}, \Psi_{A-1}^f | \Psi_A^0\rangle = \int e^{i\vec{P}_{A-1}\vec{r}_1} \Psi_{A-1}^f(\vec{r}_2 \ldots \vec{r}_A) \times \Psi_A^0(\vec{r}_1, \vec{r}_2 \ldots \vec{r}_A)\delta\left(\sum_{j=1}^A \vec{r}_j\right)\prod_{i=1}^A \mathrm{d}\vec{r}_i\,. \quad (21)$$

Because of the energy conservation

$$\nu + M_A = P_{(A-1)0} + p_{x0}\,, \quad (22)$$

where p_{x0} is the total energy of the debris, the removal energy can be written in the following way:

$$E = \nu + M - p_{x0} \quad (23)$$

if the total energy of the system $(A-1)$ is approximated by its nonrelativistic expression and the recoil energy disregarded.

As is well known [23], the integral of the spectral function over the removal energy E defines the (undistorted) momentum distributions

$$n^A(|\vec{p}|) = \int e^{-i\vec{p}(\vec{r}-\vec{r}\,')}\rho(\vec{r}, \vec{r}\,')\mathrm{d}\vec{r}\mathrm{d}\vec{r}\,' = \int \mathrm{d}E P^A(E, |\vec{p}|) = n_0^A(\vec{p}) + n_1^A(\vec{p})\,, \quad (24)$$

where

$$\rho(\vec{r},\vec{r}\,') = \int \Psi_A^{0\,*}(\vec{r},\vec{r}_2\ldots\vec{r}_A)\Psi_A^0(\vec{r}\,',\vec{r}_2\ldots\vec{r}_A)\prod_{i=2}^{A}\mathrm{d}\vec{r}_i \ , \tag{25}$$

is the one-body mixed density matrix. In eq. (24), n_0^A represents the mean-field uncorrelated momentum distribution arising from the summation over the discrete hole states of the final system, whereas n_1^A is the correlated momentum distribution resulting from the summation over high excitation states of the final system, which originate from nucleon-nucleon correlations.

In this paper we will consider semi-inclusive processes, when the cross-section (16) is integrated over the removal energy E, at a fixed value of $\vec{P}_{A-1}$. Thus, owing to

$$\sum_f \Psi_{A-1}^{f\,*}(\vec{r}_2'\ldots\vec{r}_A{}')\Psi_{A-1}^f(\vec{r}_2\ldots\vec{r}_A) = \prod_{j=2}^{A}\delta(\vec{r}_j-\vec{r}_j') \ , \tag{26}$$

the cross-section (16) becomes directly proportional to the momentum distribution $n_A(|\vec{P}_{A-1}|)$. However, since, as previously stated, we will only consider the formation of a low momentum and low excitation energy $(A-1)$ system, the summation over f is effectively limited to the hole states α of the initial nucleus, which means that the only relevant quantity is the low-momentum part of

$$n_0^A(|\vec{P}_{A-1}|) = \sum_{\alpha<F}|F_{A,A-1}^{\alpha<F}(|\vec{P}_{A-1}|)|^2 \ , \tag{27}$$

where the sum extends over the states below the Fermi sea occupied in the ground state. Following [3], let us briefly discuss the A-dependence of the cross-section (16). In this respect it should be pointed out that nuclear effects are not only generated by the nucleon momentum distribution $n_0^A(|\vec{P}_{A-1}|)$, but also by the quantities y_A and $z_1^{(A)}$, which differ from the corresponding quantities for a free nucleon ($y=\nu/E_e$ and $z_1^{(N)}=1$) if the off mass shell of the nucleon ($p_1^2\neq M^2$) generated by nuclear binding is taken into account. However, such a dependence is not only very small, but it completely disappears in the ratio between the cross-sections from nuclei A and A',

$$R_{\mathrm{Bj}}(x_{\mathrm{Bj}}/z_1^{(A)},Q^2,|\vec{P}_{A-1}|,A,A') = \frac{F_2^{N/A}(x_{\mathrm{Bj}}/z_1^{(A)},Q^2)}{F_2^{N/A'}(x_{\mathrm{Bj}}/z_1^{(A')},Q^2)}\frac{n_0^A(|\vec{P}_{A-1}|)}{n_0^{A'}(|\vec{P}_{A-1}|)} \tag{28}$$

$$\rightarrow \frac{n_0^A(|\vec{P}_{A-1}|)}{n_0^{A'}(|\vec{P}_{A-1}|)} \equiv R_{A,A'}(|\vec{P}_{A-1}\ |), \tag{29}$$

which means that in the Bjorken limit the A-dependence of the ratio R is entirely governed by the A-dependence of the nucleon momentum distribution $n_0^A(|\vec{P}_{A-1}|)$ in nuclei A and A'. Since, as shown in fig. 2, n_0^A exhibits a strong A-dependence for low values of $|\vec{P}_{A-1}|$, a plot of R *vs.* $|\vec{P}_{A-1}|$ should follow the behavior of $n_0^A(|\vec{P}_{A-1}|)$ in nuclei A and A' and the experimental observation of such a behavior would represent a stringent test of the spectator mechanism independently of the model for $F_2^{N/A}$.

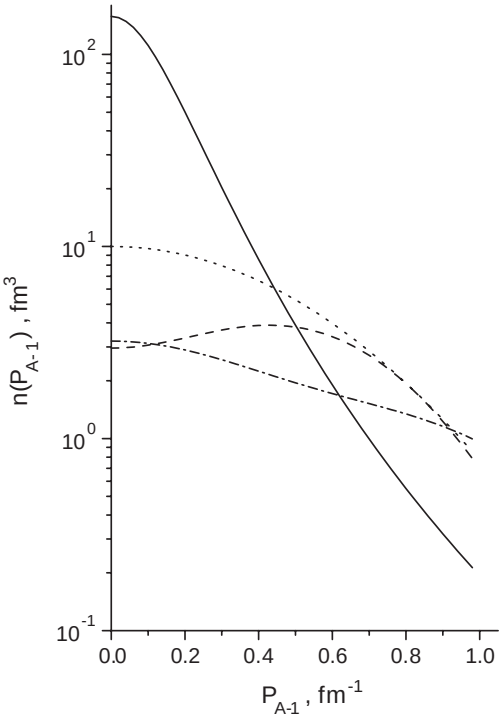

Fig. 2. The proton momentum distributions in ^{2}H (full line), ^{4}He (dotted line), ^{16}O (dashed line) and ^{40}Ca (dot-dashed line) calculated using realistic nucleon-nucleon interactions (see [3] for original references).

The expected behavior of the ratio eq. (29) for $A=2$ and different values of A' is presented in fig. 3. These results clearly show that the observation of recoil nuclei in the ground state, with a $|\vec{P}_{A-1}|$-dependence similar to the one predicted by the momentum distributions, would represent, on the one hand, an indication that the FSI between the lepto-produced hadronic states and the nuclear medium is such as to leave intact part of the final $(A-1)$ nuclei. One could hope that the number of the detected nuclei together with the momentum dependence of the cross-section could provide information on the nature and the details of the hadronization mechanism in a more sensitive way than, *e.g.*, the energy transfer dependence of the forward hadro-production in the process $A(e,e'h)X$ [4,6].

From what exhibited in this section, it should be clear that the choice of considering low momentum components and low excitation energies of the detected $(A-1)$ system, is dictated by two main reasons: i) the nucleon momentum distributions at high values of $|\vec{p}|$ scale with A, so that all advantages of having a strong A-dependence of the ratio eq. (29) would be lost; ii) the high momentum part of $n(|\vec{p}|)$ is almost entirely exhausted by $n_1(|\vec{p}|)$ which results from high values of the removal (excitation) energy of $(A-1)$ in eq. (24) ($E=E_{A-1}^f+E_{\min}\geq 50$–100 MeV); in such a case there are little chances for the final $(A-1)$ system to remain intact. Experimentally one

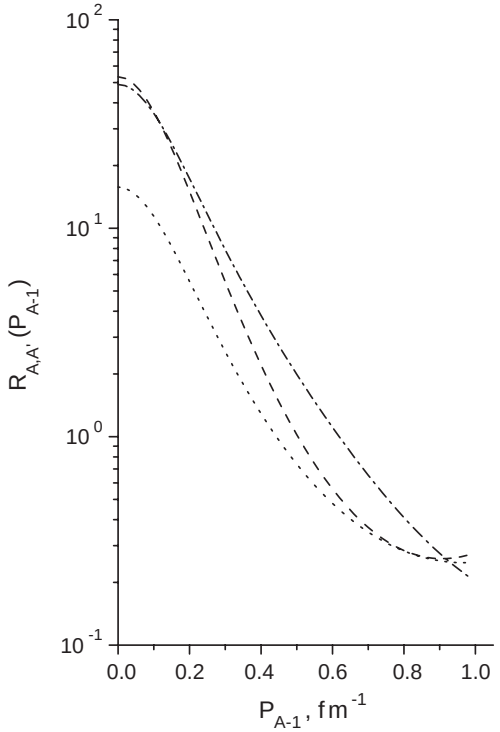

Fig. 3. The ratio $R_{A,A'}(P_{A-1})$ (eq. (29) with $P_{A-1} \equiv |\vec{P}_{A-1}|$) corresponding to $A = 2$ and $A' = 4$ (dotted line), $A' = 16$ (dashed line) and $A' = 40$ (dot-dashed line).

has therefore to look for a *bound* $(A-1)$ system in the ground state or in a state of low excitation corresponding roughly to the hole shell model states of the target ($\epsilon_\alpha^{\max} \simeq$ 30–50 MeV) (in principle, these states could be reached by the de-excitation of a highly excited state of $(A-1)$ through pion emission. These events should be excluded in the analysis, but, as explained above, they provide only a tiny contribution to the low momentum part of $n(|\vec{p}|)$). It is clear that in case of few-body targets, *e.g.* ^{2}H, ^{3}He and ^{4}He, the ambiguities deriving from the identification of $(A-1)$ as resulting from the process we are investigating are strongly reduced, for one has to detect, in coincidence with the scattered electron, a *nucleon*, a *deuteron* and ^{3}He(^{3}H), respectively.

3.2 Final-state interaction and hadronization

In this section we are going to consider the modifications of the cross-section induced by the FSI of the nucleon debris produced in the DIS on a bound nucleon. In this case, the Spectral Function has to be replaced by the *Distorted* (D) Spectral Function, which can be written in the following way:

$$P_{\rm D}^A(E,\vec{P}_{A-1}) = \sum_f |F_{A-1,A}^{f,{\rm D}}(\vec{P}_{A-1})|^2 \times \delta(E-(E_{\min}+E_{A-1}^f)) \ , \qquad (30)$$

where the transition form factor is

$$F_{A-1,A}^{f,{\rm D}}(\vec{P}_{A-1}) = \langle \vec{P}_{A-1}, \Psi_{A-1}^f S_{\rm G} | \Psi_A^0 \rangle = \int e^{i\vec{p}_{A-1}\vec{r}_1} S_{\rm G}^\dagger(\vec{r}_1 \dots \vec{r}_A) {\Psi_{A-1}^f}^*(\vec{r}_2 \dots \vec{r}_A) \times \Psi_A^0(\vec{r}_1, \vec{r}_2 \dots \vec{r}_A)\ \delta\left(\sum_{j=1}^A \vec{r}_j\right) \prod_{i=1}^A {\rm d}\vec{r}_i \ . \qquad (31)$$

The quantity $S_{\rm G}$ in eq. (31) is the Glauber operator, which describes the FSI of the debris from the struck proton with the $(A-1)$ system, *i.e.*

$$S_{\rm G}(\vec{r}_1 \dots \vec{r}_A) = \prod_{i=2}^A \left[1 - \Gamma^{N^*N}(\vec{b}_1 - \vec{b}_i, z_i - z_1)\Theta(z_i - z_1)\right] \ , \qquad (32)$$

where $\vec{b}_i$ and z_i are the transverse and longitudinal components, respectively, of the coordinate of nucleon "i", $\vec{r}_i \equiv (\vec{b}_i, z_i)$, $\Gamma^{N^*N}(\vec{b})$ is the Glauber profile function describing the elastic scattering of the debris, denoted N^*, with the nucleons of the $(A-1)$ system, and the function $\theta(z_i - z_1)$ takes care of the fact that debris of the struck proton "1" propagates along a straight-path trajectory, so that they interacts with nucleon "j" only if $z_j > z_1$. We have chosen the longitudinal axis z along the momentum of the virtual photon, and besides the usual dependence on the transverse separation $\vec{b}_1 - \vec{b}_i$ between N^* and N_i for a high-energy amplitude, we have also reserved a dependence of Γ^{N^*N} on the longitudinal separation $z_i - z_1$, which should take care of the time dependence of the effective cross-section discussed above. Let us eventually point out that because of the effects from the FSI, the Distorted Spectral Function depends now upon the vector $\vec{P}_{A-1} \neq \vec{p}_1$. With the FSI taken into account, the Distorted cross-section is now eq. (16) with $P^A(|\vec{P}_{A-1}|, E)$ replaced by $P_{\rm D}^A(E, \vec{P}_{A-1})$. The cross-section integrated over the removal energy becomes proportional to the *distorted momentum distribution*

$$n_{\rm D}^A(\vec{P}_{A-1}) = \sum_f \left| F_{A,A-1}^{f,{\rm D}}(\vec{P}_{A-1}) \right|^2 = (2\pi)^{-3} \int e^{i\vec{P}_{A-1}(\vec{r}-\vec{r}\,')} \rho_{\rm D}(\vec{r},\vec{r}\,') {\rm d}\vec{r}{\rm d}\vec{r}\,' \ , \qquad (33)$$

where

$$\rho_{\rm D}(\vec{r},\vec{r}\,') = \int {\Psi_A^0}^*(\vec{r},\vec{r}_2 \dots \vec{r}_A) S_{\rm G}^\dagger(\vec{r},\vec{r}_2 \dots \vec{r}_A) \times S_{\rm G}(\vec{r}\,',\vec{r}_2 \dots \vec{r}_A) \Psi_A^0(\vec{r}\,',\vec{r}_2 \dots \vec{r}_A) \prod_{i=2}^A {\rm d}\vec{r}_i \qquad (34)$$

is the one-body *distorted* mixed density matrix.

A general approach to calculate $\rho_{\rm D}(\vec{r},\vec{r}\,')$ has been developed in ref. [24] in terms of correlated wave functions. Since we are interested in the low momentum part

of the wave function, and also due to the exploratory nature of our calculations, we limit ourself here to a traditional Glauber-type nuclear-structure approach in which $\Psi^0_A(\vec{r}, \vec{r}_2 \ldots \vec{r}_A)$ is written as a product of a function ϕ, describing the motion of nucleon "1" and the wave function $\Psi^f_{A-1}(\vec{r}_2 \ldots \vec{r}_A)$ of the spectator, and $|\Psi^f_{A-1}(\vec{r}_2 \ldots \vec{r}_A)|^2$ is factorized into a product of single-particle densities. One obtains, in this case,

$$n^A_{\rm D}(\vec{P}_{A-1}) \equiv N(\vec{P}_{A-1}) = \left| F^{\rm D}_{A,A-1}(\vec{P}_{A-1}) \right|^2 \ , \qquad (35)$$

with

$$F^{\rm D}_{A,A-1}(\vec{P}_{A-1}) \simeq \int e^{i\vec{P}_{A-1}\,\vec{r}}\,\phi(\vec{r}) \left[1 - \frac{S(\vec{b},z)}{2(A-1)}\right]^{A-1} {\rm d}\vec{r}, \qquad (36)$$

and

$$S(\vec{b},z) = \int_z^\infty {\rm d}z'\,\rho_A(\vec{b},z')\,\sigma_{\rm eff}(z'-z) \ , \qquad (37)$$

where $\rho_A(\vec{b},z)$ is the nuclear density (normalized as $\int {\rm d}^3r\,\rho_A(\vec{r}) = A$), $\phi(\vec{r})$ describes the relative motion of the struck nucleon with respect to the spectator $(A-1)$ nucleus, and $\sigma_{\rm eff}(z'-z)$ is given by (6) or (15).

We have estimated the Distorted form factor, eq. (37), within the optical approximation, obtaining

$$F^{\rm D}_{A,A-1}(\vec{P}_{A-1}) = \int {\rm d}^2b\, e^{i\,\vec{P}_{\rm T}\,\vec{b}} \times \int_{-\infty}^{\infty} {\rm d}z\, e^{i\,P_{\rm L} z}\,\phi(\vec{b},z) \exp\left[-\frac{1}{2}\,S(\vec{b},z)\right] \ , \qquad (38)$$

where $\vec{P}_{\rm T}$ and $P_{\rm L}$ denote the transverse and longitudinal components of $\vec{P}_{A-1}$ with respect to $\vec{q}$. The optical approximation is a rather good one for heavy nuclei, but it should be abandoned in case of light nuclei for which eq. (34) has to be used.

The total cross-section of the process is proportional to the integral of the distorted transition matrix element, obtaining

$$\sigma_{\rm tot} \propto \int {\rm d}^3P_{A-1}\ \left| F^{\rm D}_{A,A-1}(P_{A-1}) \right|^2 = \int {\rm d}^2b \int_{-\infty}^{\infty} {\rm d}z\,\rho(\vec{b},z) \exp\left[-S(\vec{b},z)\right] \ . \qquad (39)$$

4 Results of the calculations of the total cross-section and the distorted momentum distributions

We have calculated both the total cross-section and the distorted momentum distribution of the process $A(e,e'(A-1))X$ off ^{4}He, ^{16}O, and ^{40}Ca; the hit nucleon is considered to be a proton. For the nuclear density $\rho_A(\vec{b},z)$ we have used both the Harmonic Oscillator and the Fermi distribution forms. As for the function $\phi(\vec{b}_1,z_1)$, which describes the relative motion of nucleon 1 and the spectator nucleus $(A-1)$, it has been chosen such that when FSI are absent, $N(|\vec{P}_{A-1}|)$ coincides with the low momentum part of the distributions given in ref. [26]. The parameters used for the calculation of the effective cross-sections (eqs. (6) and (15)) were as follows: $\sigma^{NN}_{\rm tot} = 40\,{\rm mb}$, $\sigma^{\pi N}_{\rm tot} = 20\,{\rm mb}$, $\Lambda_{\rm QCD} = 0.25\,{\rm GeV}$, $\lambda = 0.65\,{\rm GeV}$. The results of the calculations are presented in figs. 4-9.

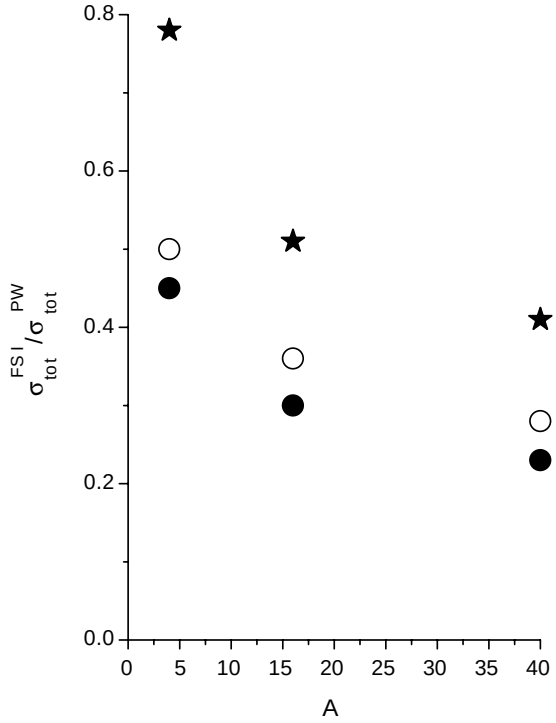

Fig. 4. The ratio between the total cross-section (eq. (39) calculated taking into account $(S(\vec{b},z) \neq 0,\ \sigma_{\rm tot} \equiv \sigma^{\rm FSI}_{\rm tot})$ and disregarding $(S(\vec{b},z) = 0,\ \sigma_{\rm tot} \equiv \sigma^{\rm PW}_{\rm tot})$ the Final-State Interaction. The open dots correspond to the effective cross-section of the nucleon debris given by the color string model (eq. (6)), whereas the full dots correspond to the cross-section where the gluon Bremsstrahlung has also been considered (eq. (15)) at $Q^2 = 100\,{\rm GeV}^2$. The stars represent the *proton* transparency calculated in refs. [24,25] for the reaction $A(e,e'p)X$.

Figure 4 shows the ratio of the distorted to undistorted total cross-sections defined by eq. (39) calculated either taking into account $(S(\vec{b},z) \neq 0)$, or disregarding $(S(\vec{b},z) = 0)$ the effect of the nucleon debris rescattering in the medium, respectively.

As anticipated, the rescattering effects exhibit a decreasing A-dependence. The effect of gluon radiation, responsible for the difference between closed and open dots, is a nearly A-independent 10% correction. We have also calculated the nuclear transparency for the reaction of quasi-elastic scattering $A(e,e'p)B$ where the intact struck proton (Glauber approximation) propagates through the nucleus. These results, depicted by star points, clearly

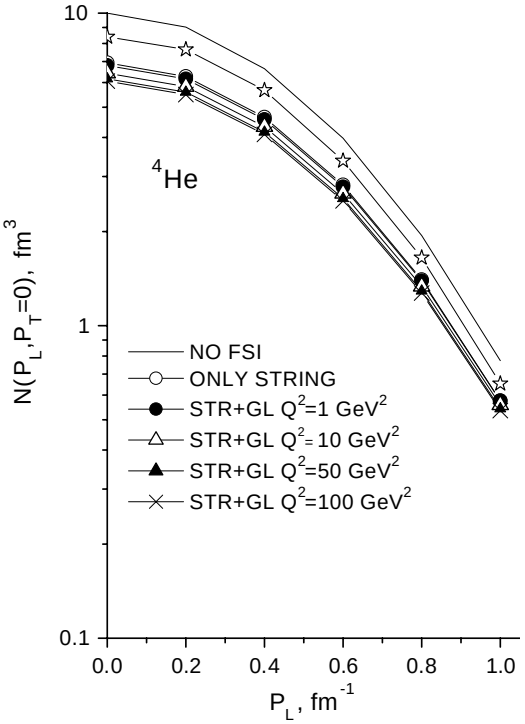

Fig. 5. The proton Momentum Distribution for ^{4}He shown in fig. 1 (NO FSI) compared with the Distorted Momentum Distribution $N(\vec{P}_{A-1})$ (eq. (35)) plotted *vs.* $P_{\rm L}$ for $P_{\rm T} = 0$. The curve labeled by open dots has been obtained using the effective cross-section for the nucleon debris corresponding to the color string model (eq. (6)), whereas the other curves correspond to the cross-section which includes also the gluon Bremsstrahlung (eq. (15)). The stars represent the distorted *proton* momentum distributions calculated in ref. [25] for the semi-inclusive process ^{4}He$(e,e'p)X$.

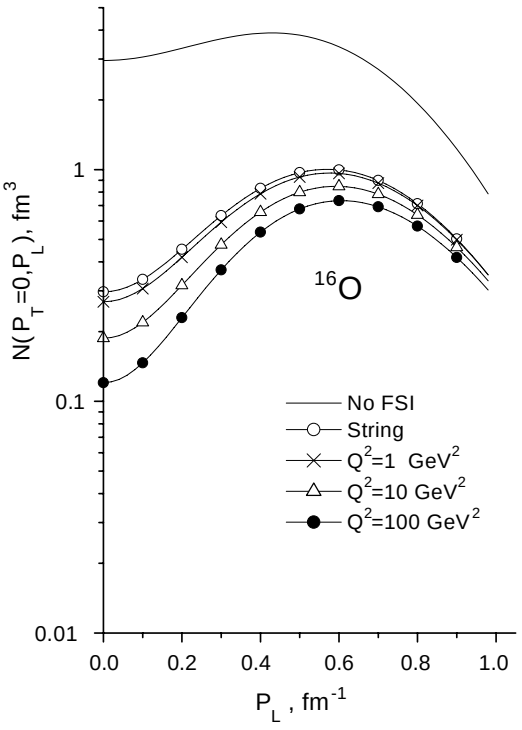

Fig. 6. The same as in fig. 5 but for ^{16}O. The *proton* rescattering in the reaction ^{16}O$(e,e'p)X$ damps the momentum distribution (full curve) by a factor of about 0.5 [25].

exhibits the expected weaker absorption effects for the proton compared to the debris in the process $A(e,e'(A-1))X$. The momentum distributions, eq. (27), for ^{4}He, ^{16}O and ^{40}Ca, are compared in figs. 5-7 with the distorted momentum distributions defined by eq. (35) calculated for $P_{\rm T} = 0$.

Concerning the results presented in these figures, the following remarks are in order:

1. Due to the smaller dimensions, rescattering effects are less important in ^{4}He than in heavier nuclei. As a matter of fact, in the former case, they simply reduce, in the considered range of momenta, to an almost constant reduction of about 50%, whereas it appears that for medium weight and heavy nuclei not only the absorption is substantially stronger, but appreciable distortion effects are apparent, with the role of gluon radiation increasing with A.
2. It is interesting to compare the process $A(e,e'(A-1))X$ we are investigating occurring at Bjorken $x \ll 1$, with the semi-inclusive *nucleon* knock-out $A(e,e'p)X$ occurring at Bjorken $x \simeq 1$ (note that X refers to the proton debris in the $A(e,e'(A-1))X$ process, and to a $(A-1)$ nucleon state in the $A(e,e'p)X$ process). Within the PW approximation the two processes are proportional to the same nuclear part, *viz* the nucleon momentum distribution $n^A(p)$ (eq. (24)), whereas when the FSI is considered, the first process will be distorted by the *nucleon debris* rescattering, and the second one by the *proton* rescattering. Thus, it appears that by comparing the two processes the differences between nucleon debris and proton propagations in the nuclear medium can be investigated. The calculation of rescattering effects in the processes ^{4}He$(e,e'p)X$, ^{16}O$(e,e'p)X$ and ^{40}Ca$(e,e'p)X$ has been performed in [25] by a Glauber-type approach and the results can be summarized as follows: in the momentum region considered in this paper, the effects of the FSI, due to the proton rescattering, damp the momentum distributions by an almost momentum-independent amount, the reduction factors being 0.85, 0.5 and 0.5 in ^{4}He, ^{16}O and ^{40}Ca, respectively. By comparing these results with the ones presented in figs. 5-7, we can conclude that, apart from ^{4}He, the effects of proton and nucleon debris propagation are, as expected, very different.

In fig. 8 the ratio $R_{A,A'}$ (eq. (29)), which is plotted in fig. 3 in the case of the PW approximation, is shown when the nucleon debris rescattering is taken into account in the final state.

It is gratifying to see that when the final-state rescattering of the debris is taken into account, the differences between different nuclei, *i.e.* nuclear effects, are even emphasized.

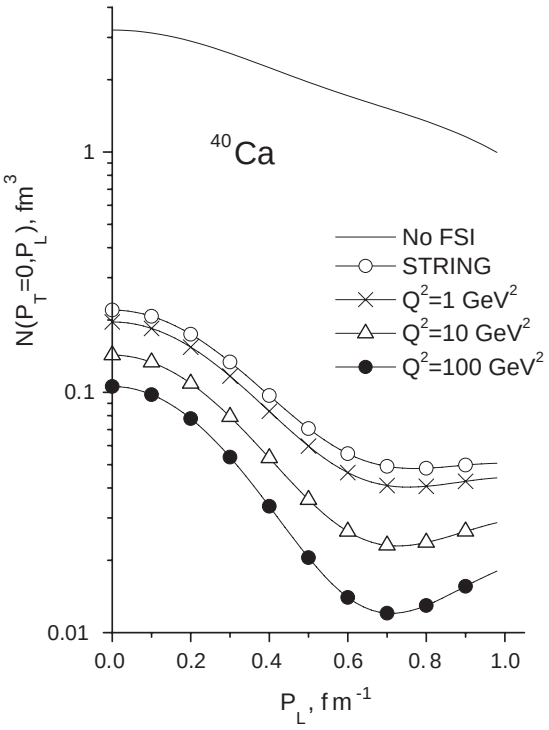

Fig. 7. The same as in fig. 5 but for ^{40}Ca. The *proton* rescattering in the reaction $^{40}\mathrm{Ca}(e,e'p)X$ damps the momentum distribution (full curve) by a factor of about 0.5 [25].

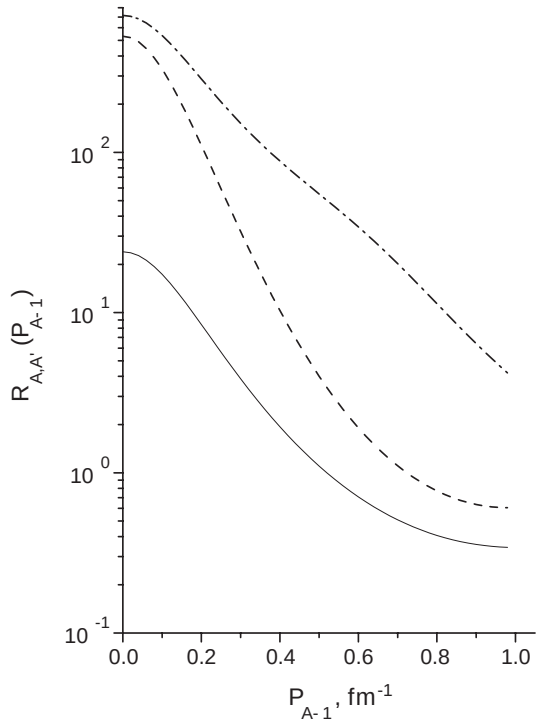

Fig. 8. The same quantity as in fig. 3 obtained with the Distorted Momentum Distributions shown in figs. 4-6 (STRING). Full line: ^{4}He; dashed line: ^{16}O; dot-dashed line: ^{40}Ca.

In fig. 9, the dependence of our results upon the choice of the function $\phi(\vec{b},z)$ describing in the target ground state the relative motion between the hit nucleon and the spectator $(A-1)$, is exhibited by comparing the results obtained with the realistic function used in the calculations with the results obtained with a simple Gaussian function. It can be seen that, apart from ^{4}He, the use of a Gaussian function is not recommended.

Eventually, in fig. 10, the sensitivity of our results upon the quantities entering the effective cross-section (eq. (15)), *viz* $\sigma_{\mathrm{tot}}^{NN}$ and $\sigma_{\mathrm{tot}}^{\pi N}$, is illustrated.

5 Summary and conclusions

In this paper we have considered a theoretical model to describe the FSI arising from the propagation and hadronization of the partonic debris produced from the hard scattering of a lepton off a nucleon bound in a nucleus A. The FSI arises due to the rescattering of the hadrons which are formed both from string breaking and from gluon radiations. In order to experimentally investigate the correctness of the model, we have analyzed the semi-inclusive process in which, instead of a secondary, *e.g.* leading, hadron, the whole $(A-1)$ nucleus in low momentum and energy states, is detected in coincidence with the scattered lepton. In absence of any FSI, the momentum distributions of the $(A-1)$ nucleus would be nothing but the momentum distributions of the hit nucleon and its integral will give the total number of surviving $(A-1)$ nuclei; when the FSI is switched on, the surviving probability will be reduced and the momentum distributions will be distorted. We have shown that both effects sensibly depend upon the details of the rescattering and hadronization of the nucleon debris. By comparing the results for the process $A(e,e'(A-1))X$ with the much investigated process of nucleon knock-out, $A(e,e'p)X$, the differences between the *nucleon* and its *debris* propagations in the nuclear environment can be investigated. For example, we have found that whereas 60% of the knocked-out protons off ^{16}O at $Q^2=1\,\mathrm{GeV}^2$ escape the nucleus without interaction, for a debris of a struck nucleon the survival probability reduces down to 25%. Furthermore, the momentum distributions of the recoiling $(A-1)$ nuclei turn out to be very sensitive to the details of the model for hadronization in nuclear environment. Up to now, information on hadron formation time and hadronization has been collected mainly from the measurement of the ratio between the semi-inclusive cross-section for the leading-hadron production for a nucleus A to that for the deuteron. This ratio increases with energy approaching 1 when the formation time of leading hadrons exceeds the nuclear size. In the process we are proposing, the effects of FSI do not vanish with energy, and vary from a factor of 2-3 in a light nucleus like ^{4}He to orders of magnitudes in heavy nuclei. Moreover, they generate peculiar and strong distortions of the nucleon momentum distributions. Thus, from a theoretical point of view, the semi-inclusive process $A(e,e'(A-1))X$ appears to be very promising, for nuclear effects not only manifest themselves in a relevant quantitative way, but also produce peculiar qualitative effects.

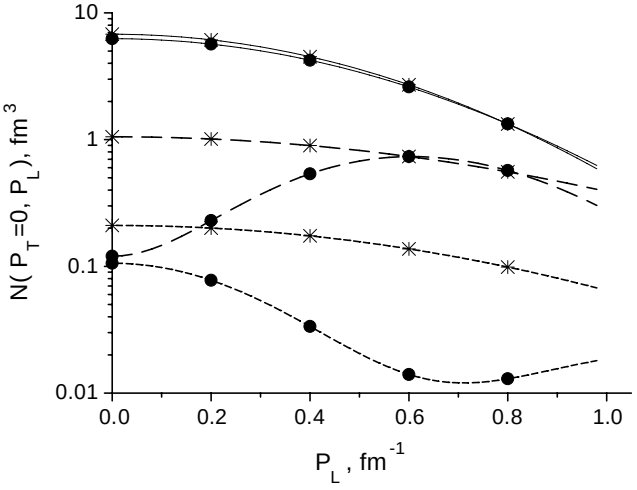

Fig. 9. The distorted momentum distributions for ^{4}He (full line), ^{16}O (long-dashed line) and ^{40}Ca (short-dashed line), calculated with two different forms for the function $\phi(\vec{b}, z)$ which describe in the target nucleus the relative motion between the hit nucleon and the spectator nucleus $(A-1)$ (cf. eq. (36)). Gaussian form: full dots; realistic form used in this paper: stars.

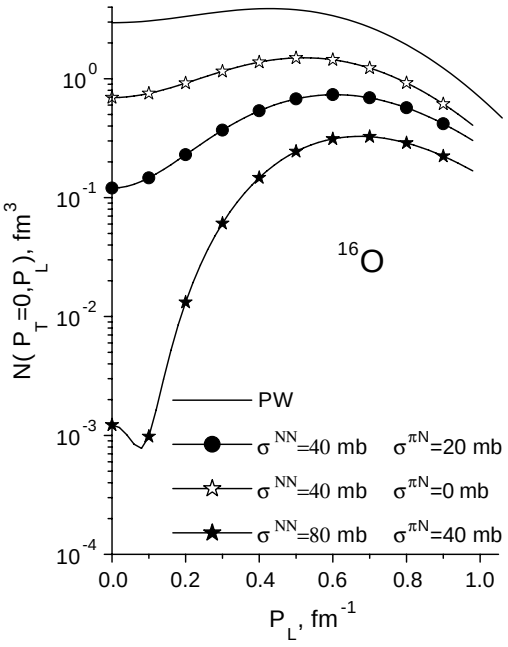

Fig. 10. The sensitivity of the distorted momentum distributions of ^{16}O upon the values of the Nucleon-Nucleon and Pion-Nucleon elementary cross-sections. The full curve represents the Plane-Wave approximation, whereas the other curves were obtained using the debris effective cross-section given by eq. (15).

An essential advantage of the process under discussion, compared to inclusive hadron production, is the possibility to study the early stage of hadronization at short formation times without being affected by cascading processes. Indeed, no cascading is possible if the recoil nucleus $(A-1)$ survives. At the same time, most of hadrons with small momentum produced in inclusive process $A(e, e'h)X$ originate from cascading of more energetic particles. In order to analyze data and extract information on the early stage of hadronization, one needs a realistic model for cascading which is barely possible.

We are grateful to D. Treleani for several fruitful discussions during the first stage of this work and to L. Kaptari for useful suggestions. CdA is indebted to B. Povh and the Max-Planck Institute für Kernphysik, Heidelberg, for several invitations which made the completion of this work possible. This work has partly been performed under the contract HPRN-CT-2000-00130 of the European Union and supported by the grant from the Gesellschaft für Schwerionenforschung Darmstadt (GSI), grant No. GSI-OR-SCH, and by the European Network *Hadronic Physics with Electromagnetic Probes*, Contract No. FMRX-CT96-0008. Partial support by the Ministero dell'Istruzione, Università e Ricerca (MIUR), through the funds COFIN01, is also acknowledged.

References

1. B. Kopeliovich, J. Nemchik, E. Predazzi, in *Future Physics at HERA*, *Proceedings of the Workshop 1995/96*, edited by G. Ingelmsan, A. De Roeck, R. Klanner, Vol. **2** (DESY, 1995/1996) p. 1038 (nucl-th/9607036).
2. B. Kopeliovich, J. Nemchik, E. Predazzi, in *Proceedings of the ELFE Summer School on Confinement Physics*, edited by S.D. Bass, P.A.M. Guichon (Editions Frontieres, Gif-sur-Yvette, 1995) p. 391 (hep-ph/9511214).
3. C. Ciofi degli Atti, L. Kaptari, S. Scopetta, Eur. Phys. J A **5**, 191 (1999).
4. L.S. Osborne *et al.*, Phys. Rev. Lett. **40**, 1624 (1978).
5. EMC Collaboration (J. Ashman *et al.*), Z. Phys. C **52**, 1 (1991).
6. HERMES Collaboration (A. Araipetian *et al.*), Eur. Phys. J. C **52**, 1 (1991).
7. HERMES Collaboration (V. Muccifora), in *Proceedings of DIS 2001, Bologna, 27 April-1 May 2001*, edited by G. Bruni, G. Iacobucci, R. Nania (World Scientific, Singapore, 2002) p. 78; Hep-ex/0106088 v1.
8. M. Arneodo, Phys. Rep. **240**, 393 (1994).
9. L.L. Frankfurt, M.I. Strikman, Phys. Rep. **160**, 235 (1988).
10. G.D. Bosveld, A.E.L. Dieperink, O. Schölten, Phys. Rev. C **45**, 2616 (1992).
11. C. Ciofi degli Atti, S. Simula, Phys. Lett. B **319**, 23 (1994); Few-Body Syst. **18**, 555 (1995).
12. A. Casher, H. Neuberger, S. Nussinov, Phys. Rev. D **20**, 179 (1979).
13. E.G. Gurvich, Phys. Lett. B **87**, 386 (1979).
14. B.Z. Kopeliovich, F. Niedermayer, Phys. Lett. B **117**, 101 (1982).
15. B.Z. Kopeliovich, F. Niedermayer, Sov. Phys. JETP **60**, 640 (1984).
16. B.Z. Kopeliovich, A. Schaefer, A.V. Tarasov, Phys. Rev. C **59**, 1609 (1999).
17. B.Z. Kopeliovich, A. Schäfer, A.V. Tarasov, Phys. Rev. D **62**, 054022 (2000) (hep-ph/9908245).
18. J. Huefner, B.Z. Kopeliovich, Phys. Lett. B **445**, 223 (1998).
19. F. Niedermayer, Phys. Rev. D **34**, 3494 (1986).

20. J.F. Gunion, G. Bertsch, Phys. Rev. D **25**, 746 (1982).
21. M. D'Elia, A. Di Giacomo, E. Meggiolaro, Phys. Lett. B **408**, 315 (1997).
22. T. Schafer, E.V. Shuryak, Rev. Mod. Phys. **70**, 323 (1998).
23. C. Ciofi degli Atti, E. Pace, G. Salmè, Phys. Lett. B **141**, 14 (1984).
24. C. Ciofi degli Atti, D. Treleani, Phys. Rev. C **60**, 24602 (1999).
25. H. Morita, C. Ciofi degli Atti, D. Treleani, Phys. Rev. C **60**, 034603 (1999).
26. C. Ciofi degli Atti, S. Simula, Phys. Rev. C **53**, 1689 (1996).